Applied Thermal Engineering 40 (2012) 80–90

Contents lists available at SciVerse ScienceDirect

Applied Thermal Engineering

journal homepage: www.elsevier.com/locate/apthermeng

Hourly performance prediction of ammonia–water solar absorption refrigeration

Muammer Ozgoren [a,*], Mehmet Bilgili [b], Osman Babayigit [c]

[a] Selcuk University, Faculty of Engineering and Architecture, Mechanical Engineering Department, 42079 Selcuklu, Konya, Turkey
[b] Cukurova University, Faculty of Ceyhan Engineering, Mechanical Engineering Department, Adana, Turkey
[c] Selcuk University, Hadim Vocational School, Konya, Turkey

ARTICLE INFO

Article history:
Received 23 February 2011
Accepted 23 January 2012
Available online 5 February 2012

Keywords:
Absorption refrigeration
COP
Evacuated tube collector
Solar radiation
Thermal energy

ABSTRACT

This paper deals with the hourly performance investigation of solar absorption refrigeration (SAR) system with evacuated tube collector and ammonia–water (NH_3–H_2O) solution. The SAR system is presented to simulate the system characteristic variations using hourly atmospheric air temperature and solar radiation data for Adana province in Turkey. The evaluation is performed for the maximum temperature occurrence day on July 29. First, the variations of various parameters, such as absorption refrigeration machine efficiency, condenser capacity and heat transfer rate in the generator and absorber during the day, are calculated for different cooling capacities and generator temperatures. Later, the minimum evacuated tube collector surface area is determined. According to the obtained results, the SAR system is considerably suitable for home/office-cooling purposes between the hours 09:00 and 16:00 in the southern region of Turkey such as Adana province. The most suitable performance of the absorption cooling system is calculated for the generator temperature values equal to or higher than 110 °C. The performance coefficient of the cooling ($COP_{cooling}$) varies in the range of 0.243–0.454 while that of the heating ($COP_{heating}$) changes from 1.243 to 1.454 during the day. Evacuated tube collector area for a 3.5 kW cooling load capacity is found to be 35.95 m^2 for the region at 16:00 whereas it is 19.85 m^2 at 12:00.

1. Introduction

Energy is considered as a major agent in the generation of wealth and an important factor in economic development [1–4]. With developing technology, the rapid increase in world population, increasing thermal loads, life standards and comfort demands in conjunction with architectural characteristics and trends, the demand for energy and its use for cooling are ever increasing [5]. In a world of continuously growing scarcity of primary energy as well as of an insurmountable irreversible environmental impact, due to human activity onto the biosphere, it is of utmost importance to look for alternatives to traditional energy sources [6]. The main advantages concern the reduction of peak loads for electricity utilities, the use of zero ozone depletion impact refrigerants, the decreased primary energy consumption and decreased global warming impact [7].

In summer, particularly under tropical climate, air conditioning has the highest energy expenditure in buildings [8]. During recent years, research aimed at the development of technologies that can offer reductions in energy consumption, peak electrical demand, and energy costs without lowering the desired level of comfort conditions has intensified. Alternative cooling technologies that can be applied to residential and commercial buildings, under a wide range of weather conditions, are being developed [9]. Reduction of energy consumption for refrigeration, however, cannot be relied solely on the improvement of efficiency. Another method of reducing the amount of energy consumption is solar cooling. Solar cooling applied in buildings is without a doubt an interesting alternative for solving problems of electrical overconsumption in traditional compression vapor air conditioning. Solar energy usage for cooling purpose in buildings offers the advantage of using an inexhaustible and free heat source to meet cooling needs most of the time [8,10]. Considering that cooling demand increases with the intensity of solar radiation, solar refrigeration has been considered as a logical solution [11].

Solar energy occupies one of the most important places among various alternative energy sources [12]. In particular, it has been identified as a convenient renewable energy source, because it is

* Corresponding author. Tel.: +90 332 223 2764; fax: +90 332 241 0635.
E-mail addresses: mozgoren@gmail.com, mozgoren@selcuk.edu.tr (M. Ozgoren), mbilgili@cu.edu.tr (M. Bilgili), obabayigit@selcuk.edu.tr (O. Babayigit).

1359-4311/$ – see front matter © 2012 Elsevier Ltd. All rights reserved.
doi:10.1016/j.applthermaleng.2012.01.058

more widely available and can be stored in batteries via photovoltaic (PV) arrays, and converted to heat or mechanical energy with reasonable efficiency [13]. The direct use of solar energy as primary energy source is interesting because of its universal availability and low environmental impact. Different technologies can be adopted to get refrigeration from solar energy: thermal and electric solar systems, and some new emerging technologies. The solar thermal systems include absorption, adsorption, solar ejector, thermo-mechanical and regenerative desiccant solutions [14]. Absorption cooling has been one of the first and oldest forms of air-conditioning and refrigeration systems since it was invented in eighteen century. Absorption systems are thermally activated, and they do not require high input shaft power. Therefore, where power is unavailable or expensive or where there is waste, geothermal, or solar heat available, absorption machines could provide reliable and quiet cooling. As no chlorofluorocarbons (CFCs) are used, absorption systems are friendlier to the environment [15–17]. In addition, they do not contribute to the ozone depletion or to global warming [18,19]. Although absorption systems seem to provide many advantages, its COP is too low and its investment cost is very expensive [20,21]. The most usual combinations of fluids include lithium bromide–water ($LiBr–H_2O$), where water vapor is the refrigerant, and ammonia–water ($NH_3–H_2O$) systems, where ammonia is the refrigerant. The $NH_3–H_2O$ system is more complicated than the $LiBr–H_2O$ system, since it needs a rectifying column to assure that no water vapor enters the evaporator, where it could freeze [22–24]. Contrary to compression refrigeration machines, which need high-quality electric energy to run, ammonia–water absorption refrigeration machines use low-quality thermal energy. The temperature of the heat source does not usually need to be so high (80–170 °C) that the waste heat from many processes can be used to power absorption refrigeration machines [9].

Turkey has high solar energy potential because of its location in the northern hemisphere with latitudes 36–42° N and longitudes 26–45° E. Yearly average solar radiation in Turkey is 3.6 kWh/m^2 day and the total yearly radiation period is ~2610 h. Solar radiation, which reaches a maximum value around noontime during summer season, can be ~900 W/m^2 in the southern region of Turkey. Consequently, it is of worth to investigate and conduct research on this solar energy source [7].

In the present study, a solar absorption refrigeration system using evacuated tube collector and $NH_3–H_2O$ absorption unit is analyzed to simulate the system by using meteorological data such as hourly atmospheric air temperature and solar radiation for Adana province in Turkey. The evaluation is performed for the maximum temperature occurrence day on July 29. The analysis reason for Adana province is that cooling season period can be extended as many as eight months and solar energy potential is fairly high level in the southern region of Turkey. Moreover, Turkish

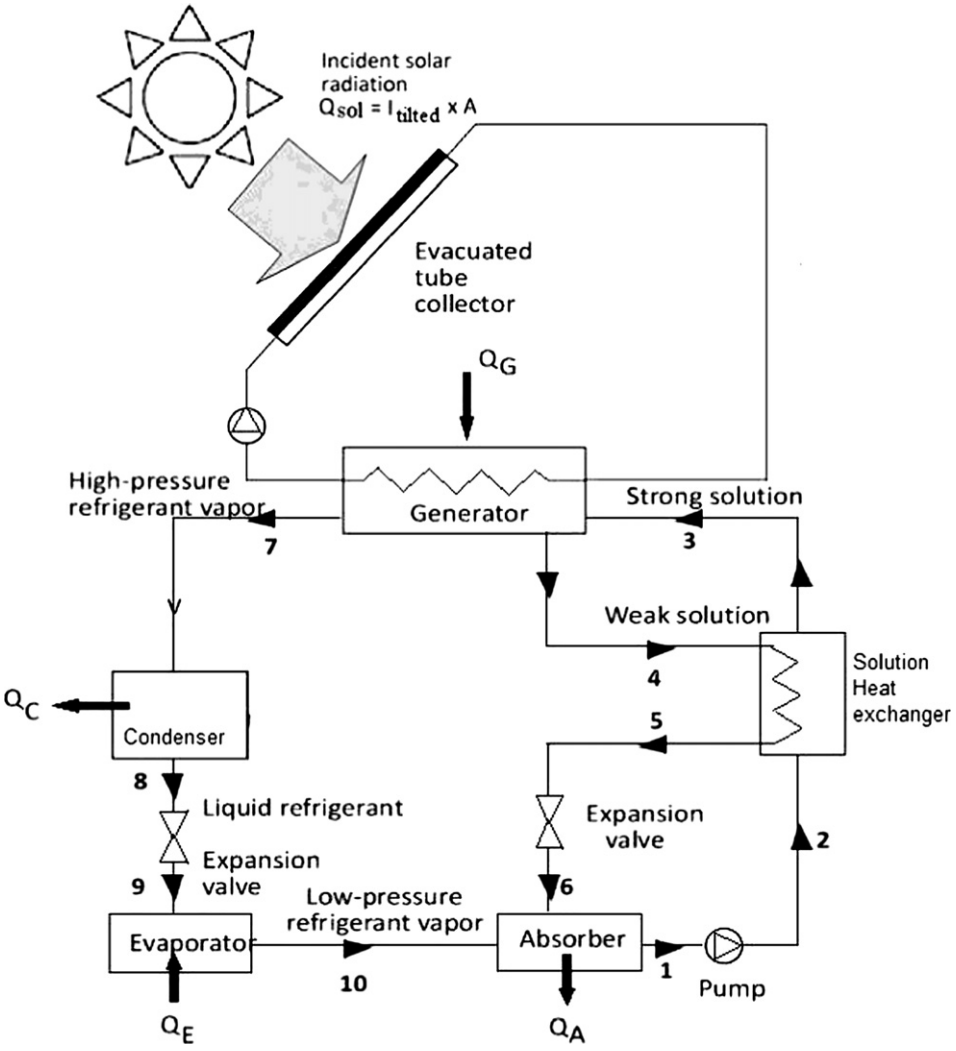

Fig. 1. Components of the solar absorption refrigeration (SAR) system.

Energy Ministry has pointed out the region as one of the promising region and hence there are a lot of solar thermal applications for hot water production and other purposes.

2. Material and methods

A schematic view of the solar absorption refrigeration (SAR) system is shown in Fig. 1. The pressure–temperature diagram of the absorption cycle is presented in Fig. 2. As shown in Fig. 1, the SAR system mainly consists of an ammonia–water (NH_3–H_2O) absorption refrigeration unit and solar thermal collectors.

2.1. Analyzing of ammonia–water absorption refrigeration system

Compared to an ordinary cooling cycle, the basic idea of an absorption system is to avoid compression work by using a suitable working pair. The working pair consists of a refrigerant (NH_3) and an absorber solution (H_2O). In absorption refrigeration system, Q_G (kW) is the heat transfer input rate from the heat source to the generator, Q_C (kW) and Q_A (kW) are the heat transfer rejection rates from condenser and absorber to the heat sinks, respectively, and Q_E (kW) is the heat input rate from the cooling load to the evaporator.

In the generator, thermal energy is added and refrigerant boils off the solution. As seen in Figs. 1 and 2, the refrigerant vapor (7) flows to the condenser, where heat is rejected as the refrigerant condenses. The condensed liquid (8) flows through an expansion valve to the evaporator (9). In the evaporator, the heat from the evaporator load evaporates the refrigerant NH_3, which flows into to the absorber (10). A small portion of the refrigerant leaves the evaporator as liquid spillover (11). At the generator exit (4), the steam consists of absorbent–refrigerant solution, which is cooled in the heat exchanger. From points 6 to 1, the solution absorbs refrigerant vapor from the evaporator and rejects heat through a heat exchanger. Due to high efficiency at high temperature, evacuated tube solar collector type has been chosen as it can provide a good performance at the high temperature required by the absorption system as stated by Assilzadeh et al. [15]. The evacuated-tube collector in which the collector surface is suspended in a glass vacuum tube is seen in Fig. 3. In this type of collector, the inside surface of the bottom half of a tube is silvered so that the solar radiation is focused on the collector surface. Because a vacuum is maintained within the collector, convection heat losses due to air movement inside the glass tube are significantly reduced [23]. Evacuated-tube collectors collect both direct and diffuse radiation so that they can operate at higher temperatures (~150 °C) than flat type collector. However, their efficiency is

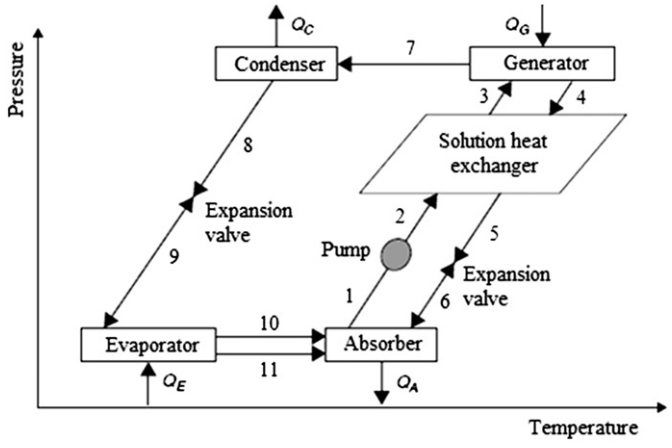

Fig. 2. The pressure–temperature diagram of absorption cycle [9].

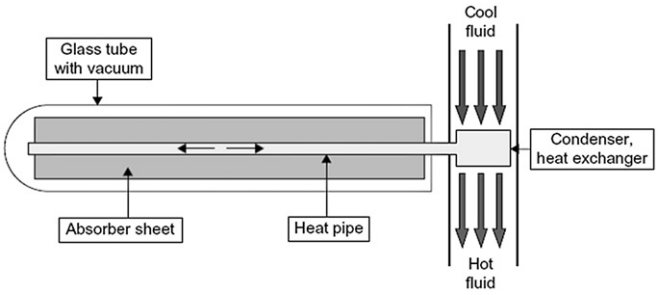

Fig. 3. Evacuated-tube solar collector [28].

higher at low incidence angles. This effect tends to give evacuated-tube collectors an advantage over flat-plate collectors in day-long performance. For this reason, this type of solar collector is more adequate for solar cooling applications [25]. The evacuated solar collectors also provide the water storage at higher temperature due to intensified energy.

For the thermodynamic analysis of the absorption refrigeration system, the principles of mass conservation and the first and second laws of thermodynamics are applied to each component of the system. Each component can be treated as a control volume with inlet and outlet streams, heat transfer and work interactions. In the system, mass conservation includes the mass balance of each material of the solution. The governing equations of mass and type of material conservation for a steady-state, steady-flow system are [9]:

$$\sum \dot{m}_i - \sum \dot{m}_o = 0 \tag{1}$$

$$\sum (\dot{m}\cdot x)_i - \sum (\dot{m}\cdot x)_o = 0 \tag{2}$$

where $\dot{m}$ (kg/s) is the mass flow rate and x is mass concentration of NH_3 in the solution. The first law of thermodynamics yields the energy balance of each component of the absorption system as follows [9]:

$$\sum (\dot{m}\cdot h)_i - \sum (\dot{m}\cdot h)_o + \left[\sum Q_i - \sum Q_o\right] + W = 0 \tag{3}$$

where h (kj/kg) is the specific enthalpy of working fluid at each corresponding state point, Q (kW) is the heat transfer and W (kW) is the pump work. In order to analyze the system in detail, mass and energy balance can be performed at each component.

At the generator, total mass balance, NH_3 mass balance and energy balance are respectively calculated by using following expressions:

$$\dot{m}_3 = \dot{m}_4 + \dot{m}_7 \tag{4}$$

$$\dot{m}_3 x_3 = \dot{m}_4 x_4 + \dot{m}_7 \tag{5}$$

$$Q_G = \dot{m}_7 h_7 + \dot{m}_4 h_4 - \dot{m}_3 h_3 \tag{6}$$

From Eqs. (4) and (5), the strong and weak solution mass flow rate can be obtained by using following expressions [26];

$$f = \frac{\dot{m}_3}{\dot{m}_7} = \frac{1 - x_4}{x_3 - x_4} \tag{7}$$

$$\frac{\dot{m}_3}{\dot{m}_7} = \frac{\dot{m}_4}{\dot{m}_7} + 1 \tag{8}$$

$$\frac{\dot{m}_4}{\dot{m}_7} = f - 1 \tag{9}$$

At the condenser, total mass balance and energy balance are calculated as follows;

$$\dot{m}_7 = \dot{m}_8 = \dot{m}_{ref} \tag{10}$$

$$Q_C = \dot{m}_{ref}(h_8 - h_7) \tag{11}$$

At the evaporator, mass balance and energy balance are determined as follows:

$$\dot{m}_9 = \dot{m}_{10} = \dot{m}_{ref} \tag{12}$$

$$Q_E = \dot{m}_{ref}(h_{10} - h_9) \tag{13}$$

At the absorber, mass balance and energy balance are given as follows:

$$\dot{m}_1 = \dot{m}_{10} + \dot{m}_6 \tag{14}$$

$$Q_A = \dot{m}_1 h_1 - \dot{m}_{10} h_{10} - \dot{m}_6 h_6 \tag{15}$$

Dividing by $\dot{m}_7$

$$q_A = f \cdot h_1 - h_{10} - (f-1) \cdot h_6 \tag{16}$$

where q_A (kj/kg) represents the heat dissipated per unit mass and f is the mass flow ratio. The first term of the right hand side represents the phase change, and the second term is the cooling of the mixture [26]. An overall energy balance of the system requires that the sum of the generator, evaporator, condenser, and absorber heat transfer rate eliminate each other and must be 0. If the absorption system model assumes that the system is in a steady-state and that the pump work and environmental heat losses are neglected, the energy balance can be written as [9]:

$$Q_C + Q_A = Q_G + Q_E \tag{17}$$

The cooling coefficient of performance (COP) of the absorption system is defined as the heat load in the evaporator per unit of heat load in the generator and can be written as [9,26]:

$$COP_{cooling} = \frac{Q_E}{Q_G} = \frac{\dot{m}_{10} h_{10} - \dot{m}_9 h_9}{\dot{m}_7 h_7 + \dot{m}_4 h_4 - \dot{m}_3 h_3} \tag{18}$$

The heating COP of the absorption system is the ratio of the combined heating capacity, obtained from the absorber and condenser, to the heat added to the generator and can be written as:

$$COP_{heating} = \frac{Q_C + Q_A}{Q_G} = \frac{(\dot{m}_8 h_8 - \dot{m}_7 h_7) + (\dot{m}_1 h_1 - \dot{m}_{10} h_{10} - \dot{m}_6 h_6)}{\dot{m}_7 h_7 + \dot{m}_4 h_4 - \dot{m}_3 h_3} \tag{19}$$

Therefore, from Eq. (17), the COP for heating can be also written as

$$COP_{heating} = \frac{Q_G + Q_E}{Q_G} = 1 + \frac{Q_E}{Q_G} = 1 + COP_{cooling} \tag{20}$$

Eq. (20) shows that the heating COP for all cases is greater than the cooling COP. The ideal cooling and heating coefficients of performance of the absorption system are defined with Eqs. (21) and (22), respectively. Here T_C (K), T_G (K), and T_E (K) are respectively the condenser, generator and evaporator temperatures.

$$COP^{ideal}_{cooling} = \frac{T_E}{T_G}\left(\frac{T_G - T_C}{T_C - T_E}\right) \tag{21}$$

$$COP^{ideal}_{heating} = \frac{T_C}{T_G}\left(\frac{T_G - T_E}{T_C - T_E}\right) \tag{22}$$

2.2. Analyzing of the evacuated tube solar collector

Solar thermal systems use solar heat effect rather than solar electricity to produce cooling effect. Solar thermal collectors that are available in different types and in a wide range of efficiency convert sunlight into heat and this heat in turn drives a heat-driven refrigeration machine. A solar collector provides heat to the “heat engine” or “thermal compressor” in a heat-driven refrigeration machine. A solar thermal system is designed in consideration of these two opposing trends. Depending on its optical design, a solar collector can be classified into concentrating (i.e. evacuated collectors) or non-concentrating type collector (i.e. flat-plate solar collector).

Conventional simple flat-plate solar collectors were developed for use in sunny and warm climates. Their benefits, however, are greatly reduced when conditions become unfavorable during cold, cloudy, and windy days. Furthermore, weathering influences, such as condensation and moisture, cause early deterioration of internal materials, resulting in reduced performance and system failure. On the other hand, evacuated tube collectors have less heat loss and better performance at high temperatures because of the fact that they operate differently than the other collectors available on the market [23,25]. They use compressed liquid or liquid–vapour phase change materials to transfer heat at high efficiency. They are typically made in a glass tube design, i.e. a metallic absorber inserted in an evacuated glass tube to withstand the pressure difference between the vacuum and the atmosphere. Each tube contains a glass outer tube and inner glass or metal tube attached to a fin as the absorber. Air is removed, or evacuated, from the space between the two tubes to form a vacuum, which eliminates conductive and convective heat loss as recorded by Kalogirou [25,27], Yamankaradeniz et al. [26] and Beggs [28]. Because no evaporation or condensation above the phase-change temperature is possible, the heat pipe offers inherent protection from freezing and overheating. This self-limiting temperature control is a unique feature of the evacuated heat pipe collector [27]. At collector inlet temperatures above 45 °C, and at low levels of solar radiation, the evacuated tube collectors are more efficient. However, the solar collector in a solar domestic hot water system only operates at 45 °C when the solar storage tank is already hot. Furthermore, at low levels of solar radiation there is not much solar energy available, regardless of the efficiency of the solar collector [29].

In Fig. 1, a solar collector receives solar radiation Q_{sol} (kW) that is product of the surface area A (m^2), and the solar radiation perpendicular to the tilted surface I_{tilted} (kW/m^2) from the sun and supplies $Q_{sol\text{-}gen}$ (kW) to a generator. It is assumed for the calculation that the evacuated solar collector surface is placed with tilted angle of 23° and oriented to the south direction. The ratio of supply heat $Q_{sol\text{-}gen}$ to the solar radiation production Q_{sol} is defined as the thermal efficiency of a solar thermal collector, η [30–33];

$$\eta = \frac{Q_{sol-gen}}{Q_{sol}} \tag{23}$$

The solar radiation production on collector surface area and the heat output from solar collectors can be determined using the Hottel–Whillier equation [11,28]:

$$Q_{sol} = I_{tilted} \cdot A \tag{24}$$

$$Q_{sol-gen} = F \cdot A[(\tau\alpha) I_{tilted} - U(T_W - T_A)] \tag{25}$$

where τ is the transmission coefficient, α is the absorption coefficient, U is the overall heat transfer coefficient (W/m^2 K), F is the solar-collector efficiency factor, T_W is the mean water temperature (°C) and T_A is the ambient air temperature (°C). The efficiency of a solar collector is determined by using Eqs. (24) and (25):

$$\eta = F(\tau\alpha) - \frac{FU(T_W - T_A)}{I_{tilted}} \tag{26}$$

It is possible to greatly improve solar collector efficiency by using evacuated-tube collectors. Typical values of $\tau\alpha$ and U for the evacuated tube collector are commonly taken as 0.84–0.86 and 0.8 W/m^2 K, respectively [28,34].

3. Results and discussion

3.1. Hourly climatic data

The climatic data used in this study were observed at Adana meteorological station situated in the south of Turkey's Mediterranean Region. This station is located on the geographical coordinates of 37°03″ North latitude and 35°21″ East longitude. It is located at an altitude of 27 m above sea level. The hourly climatic data for this station were measured by the Turkish State Meteorological Service (TSMS). The symbols I and I_{tilted} represent the solar radiation on horizontal and tilted collector surfaces, respectively. The measured climatic data consist of hourly records of solar radiation I (kW/m^2) and atmospheric air temperature T_A (°C) in the year 2007. Hourly values of the solar irradiation and atmospheric air temperature during the days and year are presented with three dimensional type diagrams in Fig. 4a. As seen, the solar irradiation increases with sunshine and it takes its maximum values during noon. Later, it decreases with lessening effect of the solar energy during the evening hours or later. Measurement results of solar radiation values before sunshine and after sunset are zero. Variations of the solar radiation and atmospheric air temperature for all of the day are very similar but their magnitudes are different and very fluctuated day by day. Both the solar radiation and atmospheric air temperature take their maximum values during spring and summer seasons where the cooling requires for comfort condition. The maximum hourly mean temperature happens in July. The maximum temperature occurrence day of July month is determined as 29th. For July 29, the hourly mean solar radiation on tilted evacuated tube collector surface at 23° and atmospheric air temperature are presented in Fig. 4b. The hourly atmospheric air temperature variation during the day considerably has wide range and the lowest temperature occurs between 05:00 and 06:00. On the other hand, atmospheric temperature reaches the highest value from 13:00 to 14:00 and then it decreases again. The hourly atmospheric air temperature varies from 25.9 °C to 42 °C.

The solar radiation has a variation along the daytime (i.e. from 05:00 to 19:00). As shown in Fig. 4b, there is no solar energy effect between the hours 19:00 and 04:00 (i.e. evening hours). The maximum solar radiation value (I_{tilted}) occurs at 13:00 with a magnitude of 0.719 kW/m^2. When the maximum value of atmospheric air temperature and solar radiation is compared, the maximum atmospheric air temperature is determined along the hours (13:00–14:00) while the maximum solar radiation is calculated between the hours 12:00 and 13:00.

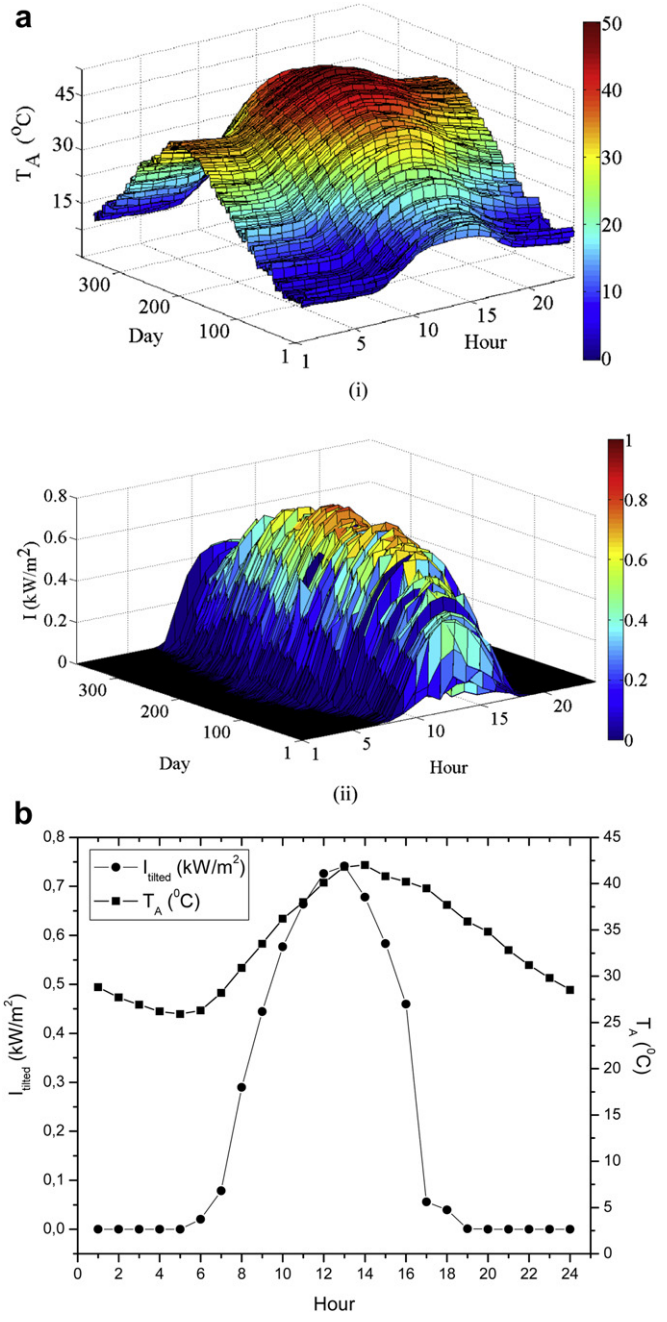

Fig. 4. a) Hourly and daily variations of (i) atmospheric air temperature and (ii) solar radiation on the horizontal surface during the days and year for Adana province. b) Hourly solar radiation intensity on tilted evacuated tube collector surface at 23° and atmospheric air temperature for Adana province on July 29.

3.2. System description

The SAR system can be considered for two related processes: to provide refrigeration for food and medicine preservation etc. and to provide comfort cooling. As well known, heat can be used for heating and cooling purpose along the year for many applications. For example, hot water produced by rejecting heat from the absorption refrigeration condenser can be used to meet hot water need of the labors for shower at any industry, mess hall need at any industry, to meet floor heating need purpose for example in a swimming pool, to supply cloth or dish washer machine hot water need and any other need. As shown in Fig. 1, the collector receives

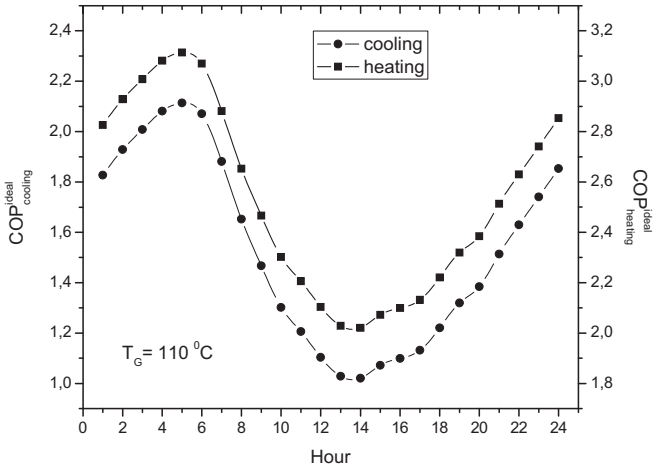

Fig. 5. Hourly variations of the ideal COPs of the absorption refrigeration system.

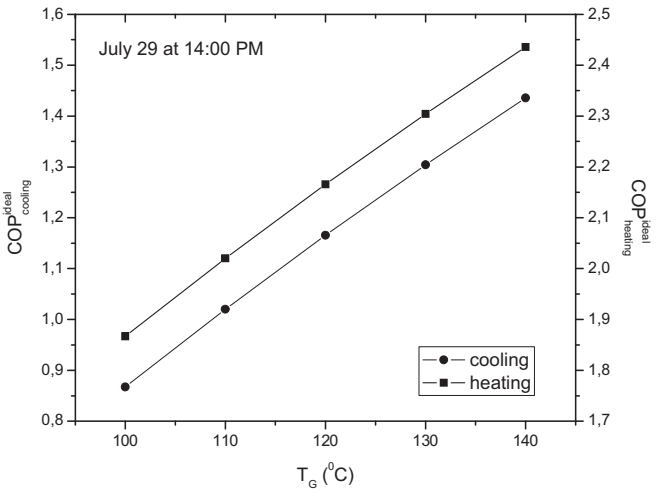

Fig. 7. Variations of the ideal COPs of the absorption refrigeration system depending on the generator temperature.

energy from sunlight. The energy is then transferred through high temperature energy storage reservoir to the refrigeration system. In the absorption system, the working pair consists of a refrigerant and an absorbent. An ammonia–water (NH_3–H_2O) solution is used as working pair, with the ammonia and water being the refrigerant and absorbent, respectively. Absorption systems are similar to vapor-compression air-conditioning systems but differ in the pressurization stage. In general, an absorbent, on the low-pressure side, absorbs an evaporating refrigerant. Compared to an ordinary cooling cycle, the basic idea of an absorption system is to avoid compression work. This is done by using a suitable working pair: a refrigerant and a solution that can absorb the refrigerant. The single-stage ammonia–water absorption refrigeration system cycle consists of four main components such as condenser, evaporator, absorber, and generator. Other auxiliary components include expansion valves, pump, rectifier and heat exchanger.

Assumptions for the calculation of the SAR system, in detail, are as follows: There are steady-state conditions. The work done by an isentropic pump, pressure drops and heat losses in components and tubes are negligible. Saturated solution leaves the absorber and generator. There is saturated refrigerant at the condenser and evaporator outlets. The flow through the adiabatic expansion valves is isenthalpic. Outlet temperature of NH_3 from generator is assumed as 110 °C and evaporation temperature is taken as 10 °C.

Condenser and absorber are cooled from the same source and therefore their temperatures are hypothesized to be same. The condensing temperature (T_C) could be commonly taken as 10 °C greater than the atmospheric air temperature (T_A). That is, $T_C = T_A + 10$ °C [26,35–38]. In order to cover daily variation of heat gain, the cooling capacity of the system (Q_E) is taken as 2.5, 3.0, 3.5 and 4.0 kW. The transmission-absorption coefficient $\tau\alpha$ and the overall heat transfer coefficient U are considered as 0.86 and 0.8 W/m^2 K, respectively [28,40]. Optimum incidence angle of the photovoltaic (PV) collector along the cooling season in this city located in the southern region of Turkey could be taken as 23° as suggested by Ersoy et al. [39]. After that, the total solar radiation intensity incident upon the collector surface at 23° was calculated from the meteorological data as defined by Duffie and Beckman [40], Ozgoren et al. [41] Jacovides et al. [42] and Notton et al. [43]. For 29th day of July, the hourly average values of atmospheric air temperature along with the solar radiation upon the collector surface at 23° are given in Fig. 4b. For example, the amounts solar radiation on 29th day of July incident upon the horizontal collector surface and tilted collector surface with 23° angle are respectively determined as 662.91 W/m^2 and 678.02 W/m^2 at 14:00. it is seen

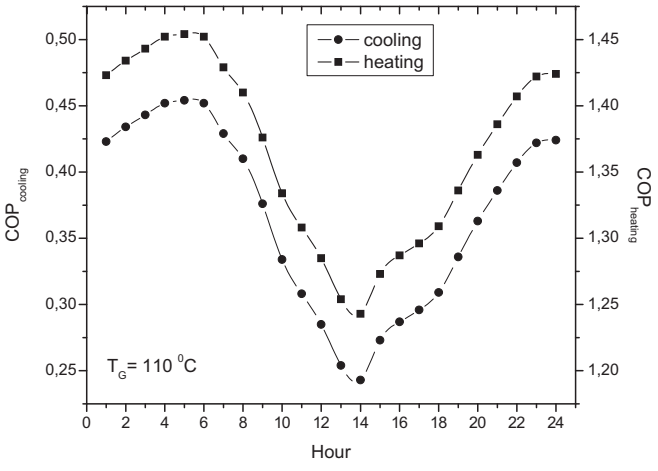

Fig. 6. Hourly variations of the COPs of the absorption refrigeration system.

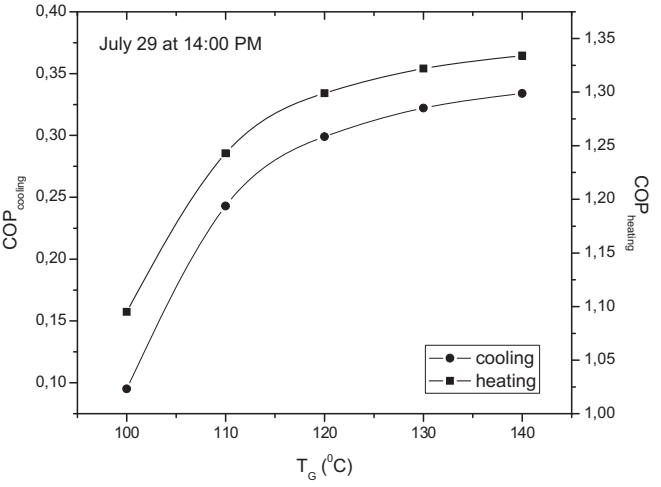

Fig. 8. Variations of the COPs of the absorption refrigeration system depending on the generator temperature.

that solar radiation value on the tilted surface increases from 10:00 to 15:00 while the remaining time of the day it slightly decreases due to the solar collector direction toward the south.

3.3. Variation of absorption refrigeration machine efficiency

Fig. 5 shows the hourly variations of the $COP_{cooling}^{ideal}$ and $COP_{heating}^{ideal}$ for $T_G = 110\,^{\circ}C$. The hourly variations of cooling and heating coefficients of performance ($COP_{cooling}$ and $COP_{heating}$) of the absorption refrigeration system were calculated in terms of the hourly atmospheric air temperature values and presented in Fig. 6. As shown in figures, the COPs fairly change during the day, the $COP_{cooling}$ is in the range of 0.243–0.454 while the $COP_{heating}$ varies from 1.243 to 1.454. The $COP_{cooling}$ value becomes the maximum value during the morning hours, later it decreases until 14:00 and then it begins to increase again. The reason of the lower $COP_{cooling}$ values around noon hours is that atmospheric air temperature (T_A) takes its higher values during this period. One of the most important affecting parameter for the $COP_{cooling}$ of the absorption refrigeration system is the atmospheric air temperature. The $COP_{cooling}$ is inversely proportional to the atmospheric air temperature.

Depending on the generator temperature, Fig. 7 displays the variations of the $COP_{cooling}^{ideal}$ and $COP_{heating}^{ideal}$ while Fig. 8 shows the variations of the $COP_{cooling}$ and $COP_{heating}$. Calculations concerning with these two figures are performed for the maximum temperature occurrence day on July 29 at 14:00. As it is seen, all of the COP values decrease with decreasing generator temperature.

3.4. Variation of condenser capacity

The hourly variations of the condenser capacity (Q_C) for different cooling capacities at the generator temperature value of 110 °C are given in Table 1. The condenser capacity of the absorption cooling system is not considerably changing during the day. According to the obtained results of the cooling loads for 2.5, 3.0, 3.5 and 4.0 kW, daily mean condenser capacity values are respectively determined as 3.02, 3.62, 4.23 and 4.83 kW. It is demonstrated that the condenser capacity of the system is directly increasing with increasing cooling capacity. The condenser capacity is in the range of 4.20–4.30 kW for the cooling capacity value of 3.5 kW. The minimum condenser capacity with a value of 4.20 kW occurs during the noon.

Table 1
Hourly variation of the condenser capacity (Q_C) for different cooling capacities (Q_E) at $T_G = 110\,^{\circ}C$.

Hour	Q_C (kW)			
	$Q_E = 2.5$ kW	$Q_E = 3.0$ kW	$Q_E = 3.5$ kW	$Q_E = 4.0$ kW
1	3.032	3.639	4.245	4.851
2	3.043	3.652	4.261	4.869
3	3.057	3.668	4.279	4.890
4	3.068	3.682	4.295	4.909
5	3.072	3.687	4.301	4.916
6	3.066	3.680	4.293	4.906
7	3.037	3.644	4.252	4.859
8	3.011	3.613	4.215	4.817
9	3.007	3.608	4.210	4.811
10	3.004	3.605	4.206	4.807
11	3.002	3.603	4.203	4.803
12	2.999	3.599	4.199	4.799
13	2.997	3.597	4.196	4.796
14	2.997	3.596	4.196	4.795
15	2.999	3.598	4.198	4.798
16	2.999	3.599	4.199	4.799
17	3.000	3.600	4.200	4.800
18	3.002	3.603	4.203	4.804
19	3.005	3.605	4.206	4.807
20	3.006	3.607	4.208	4.809
21	3.008	3.609	4.211	4.812
22	3.009	3.611	4.212	4.814
23	3.024	3.629	4.234	4.839
24	3.034	3.641	4.248	4.855

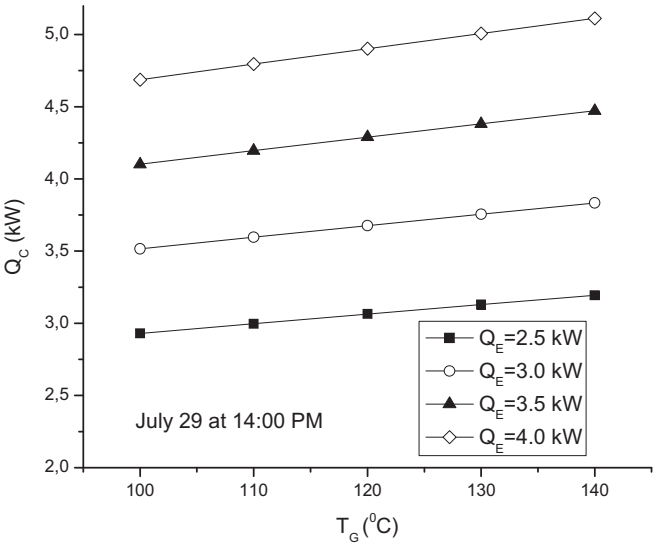

Fig. 9. Variation of the condenser capacity depending on the generator temperature.

Fig. 9 shows the variation of the condenser capacity (Q_C) depending on the generator temperature for the maximum temperature occurrence day on July 29 at 14:00. The condenser capacity is directly proportional to the generator temperature. For example, according to the $Q_E = 3.5$ kW, the condenser capacities for the generator temperature values of $T_G = 100\,^{\circ}C$ and $T_G = 140\,^{\circ}C$ are respectively calculated as 4.10 kW and 4.47 kW.

3.5. Variation of the heat transfer in the generator

Fig. 10 shows the hourly variation of the heat transfer in the generator (Q_G) for different cooling capacities at the generator

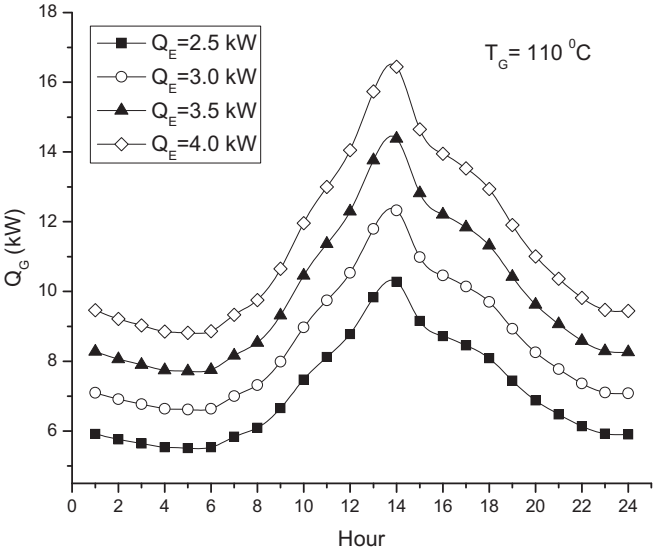

Fig. 10. Hourly variation of the heat transfer rate in the generator for different cooling capacities.

Table 2
Variation of the heat transfer in the generator (Q_G) according to the generator temperature at 14:00.

T_G (°C)	Q_G (kW)			
	$Q_E = 2.5$ kW	$Q_E = 3.0$ kW	$Q_E = 3.5$ kW	$Q_E = 4.0$ kW
100	26.24	31.49	36.74	41.99
110	10.28	12.33	14.39	16.44
120	8.35	10.02	11.70	13.37
130	7.76	9.31	10.86	12.41
140	7.49	8.99	10.49	11.98

Table 3
Variation of the heat transfer in the absorber (Q_A) according to the generator temperature at 14:00.

T_G (°C)	Q_A (kW)			
	$Q_E = 2.5$ kW	$Q_E = 3.0$ kW	$Q_E = 3.5$ kW	$Q_E = 4.0$ kW
100	25.81	30.97	36.14	41.30
110	9.78	11.73	13.69	15.65
120	7.79	9.35	10.91	12.46
130	7.13	8.55	9.98	11.40
140	6.80	8.15	9.51	10.87

temperature value of 110 °C. The required heat power in the generator of the absorption cooling system considerably varies during the day. Heat transfer rate in the generator increases with increasing cooling capacity. For example, the necessary heat transfer rates in the generator for the cooling capacity value of 2.5 and 4.0 kW at 14:00 are found to be 10.28 kW and 16.44 kW, respectively. Their minimum values occur at 5:00 (i.e. sunshine hour) for all of the evaporator capacities. After 5:00, the heat transfer rate increases proportionally with increasing atmospheric air temperature and it takes its maximum value at 14:00. In a similar way, the heat transfer rate decreases with decreasing atmospheric air temperature. The obtained results for the cooling capacity of 3.5 kW show that the heat transfer rate in the generator of the system changes from 7.72 kW to 14.39 kW during the day. The maximum condenser capacity is found to be 14.39 kW at 14:00.

Table 2 gives the variation of the heat transfer in the generator (Q_G) depending on the generator temperature. According to the obtained results for 14:00, the required power demand in the generator increases considerably when the generator temperature is lower than 110 °C. Therefore, it is demonstrated that the most suitable performance of the absorption cooling system is calculated for the generator temperature values higher than 110 °C and for the maximum atmospheric air temperature time such as during noon.

3.6. Variation of the heat transfer in the absorber

Fig. 11 shows hourly variation of the heat transfer rate in the absorber (Q_A) for different cooling capacities. Table 3 gives the variation of the heat transfer rate in the absorber (Q_A) depending on the generator temperature. In the absorption cooling system, the temperature of the water increased in the generator is lowered in the absorber by means of transferring heat to the atmosphere. Therefore, heat transfer amount in the absorber depends on the heat transfer rate taken by water and atmospheric air temperature. As seen in Fig. 11, heat transfer rate to the environment in the absorber section of the system for the generator temperature value of 110 °C varies fairly much during the day. This variation shows similar trends for all of the evaporator capacities and the heat energy variation of the given generator temperature. As cooling demand increases, heat transfer rate in the generator directly increases with releasing the heat to the atmosphere and it becomes the maximum at 14:00. For the proposed system cooling capacity 3.5 kW, heat transfer rate in the absorber of the system varies between 6.92 kW and 13.69 kW during the day.

3.7. Determination of the required collector surface area

The required collector surface area (A) of the absorption cooling system should be determined to provide enough solar energy (Q_G) for the generator of the cooling system. In order to find the collector surface area depending on the different evaporator capacities, hourly-calculated thermal power values (Q_G) are divided by global solar irradiation (I_{tilted}) and the results are presented in Fig. 12. According to the obtained results, the required collector area increases with increasing evaporator capacity as expected. However, the required collector area is calculated as higher values during the morning and evening hours while requiring the lower areas during the noon because of the highest global solar irradiation amount (I_{tilted}). It becomes fairly large area at 8:00 and 17:00

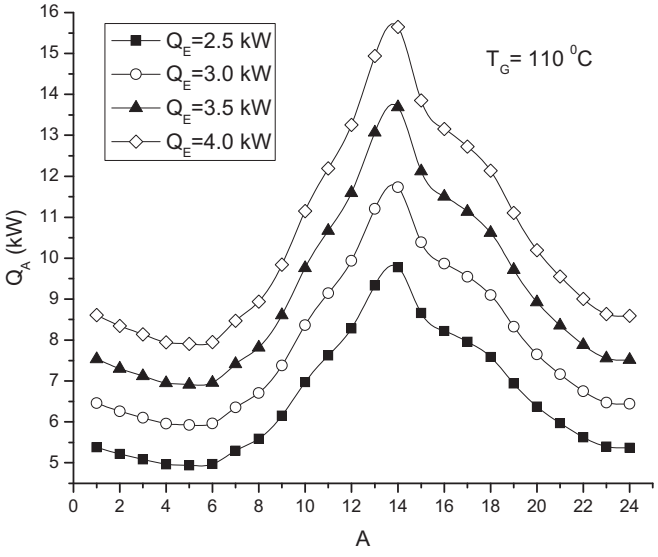

Fig. 11. Hourly variation of the heat transfer in the absorber for different cooling capacities.

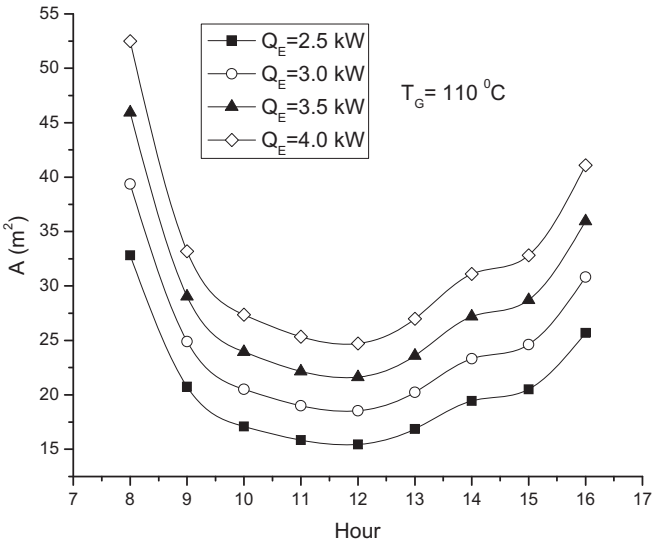

Fig. 12. Hourly variation of the required collector surface area for different cooling capacities.

Table 4
Variation of the required collector surface area (A) according to the generator temperature at 14:00.

T_G (°C)	A (m^2)			
	$Q_E = 2.5$ kW	$Q_E = 3.0$ kW	$Q_E = 3.5$ kW	$Q_E = 4.0$ kW
100	48.89	58.67	68.45	78.23
110	19.44	23.32	27.21	31.10
120	16.04	19.25	22.46	25.67
130	15.13	18.16	21.18	24.21
140	14.84	17.81	20.78	23.75

due to the lower solar irradiation and solar collector efficiency. Therefore, the solar irradiation can specially provide more benefits from 9:00 to 16:00. The required collector area for the evaporator capacity of 2.5 kW is determined as 25.68 m^2 at 16:00. The required collector areas for the evaporator capacities of 3.0, 3.5 and 4.0 kW at 16:00 are, in sequence, calculated as 30.82, 35.95 and 41.09 m^2. However, the requirement of the minimum collector area for all evaporator capacities is determined at 12:00 while the solar radiation occurs at higher values.

Table 4 presents the variation of required collector surface area with respect to the generator temperature for 14:00. The required collector surface area decreases with increasing the generator temperature of the absorption cooling system. The economic feasibility and performance of the system are better for the higher generator temperature value of 110 °C. For example, the results for the evaporator capacity of 3.5 kW, the solar collector surface area increases from 27.21 to 68.45 m^2 when the generator temperature decreases from 110 °C to 100 °C.

3.8. Variation of the solar collector efficiency, solar radiation production and the heat output from solar collector

The useful solar energy generation (Q_{sol}) is calculated by using hourly solar irradiation values (I) taken from the Turkish Meteorology Office, different evaporator capacities (Q_E) and required collector surface areas (A). Fig. 13 shows the hourly variation of the solar radiation production (Q_{sol}) for different cooling capacities. The solar collector efficiency (η) should be determined in order to calculate the heat output amount from solar collector ($Q_{sol\text{-}gen}$). The hourly variation of the evacuated solar collector efficiency (η) is

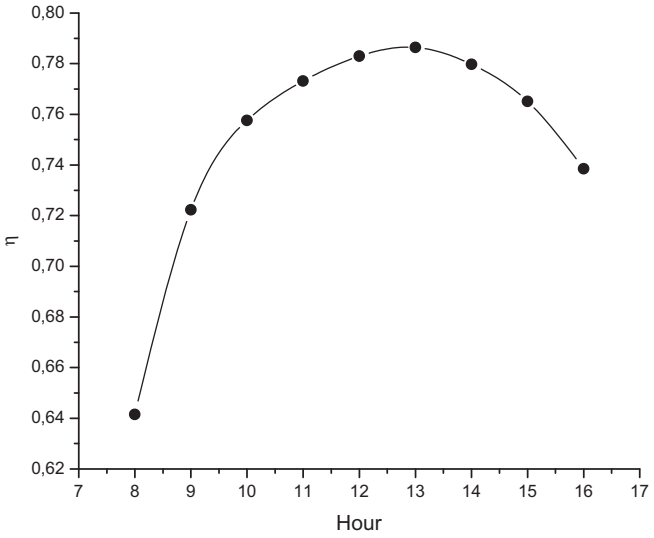

Fig. 14. Hourly variation of the solar collector efficiency.

calculated and given in Fig. 14. It varies between 0.642 and 0.786 while the solar irradiation is more effective during the hours from 08:00 to 16.00. Solar collector efficiency takes lower values during morning hours due to the lower solar irradiation while increasing with increasing solar irradiation intensity during the noon. Therefore, the solar efficiency is calculated as 0.786 at 13:0 that is the maximum value for the solar irradiation intensity of 0.719 kW/m^2. Fig. 15 shows the hourly variation of the heat output amount from solar collector ($Q_{sol\text{-}gen}$) for different cooling capacities. As seen in Fig. 15, the magnitude of $Q_{sol\text{-}gen}$ increases with increasing solar radiation and then it decreases again owing to decreasing solar energy amount.

3.9. Comparison of the heat transfer in the generator and heat output from solar collector

Comparison between the required heat transfer rate in the generator (Q_G) and heat production from solar collector ($Q_{sol\text{-}gen}$) during the day for $Q_E = 3.5$ kW is demonstrated in Fig. 16. As seen in

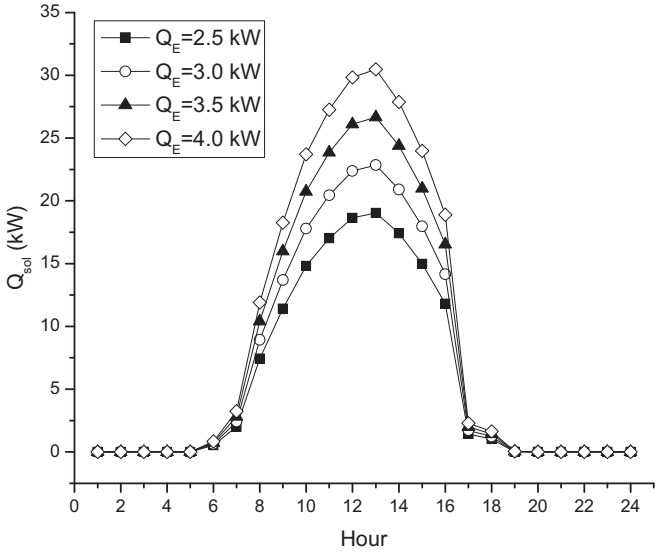

Fig. 13. The hourly variation of the solar radiation production for different cooling capacities.

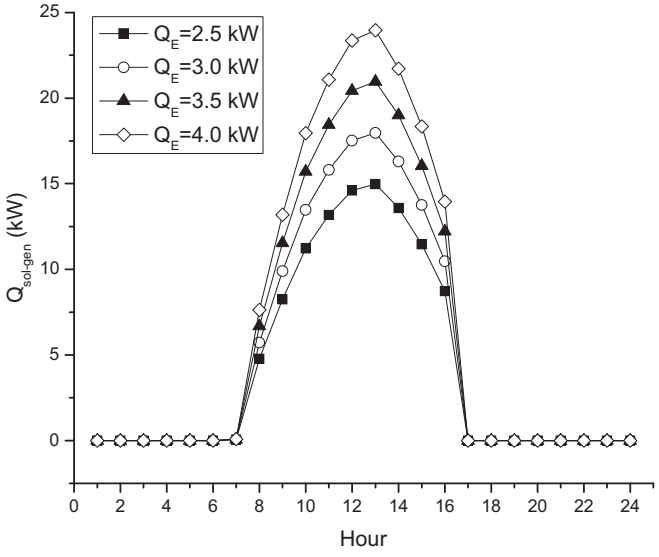

Fig. 15. The hourly variation of the heat output from the solar collector for different cooling capacities.

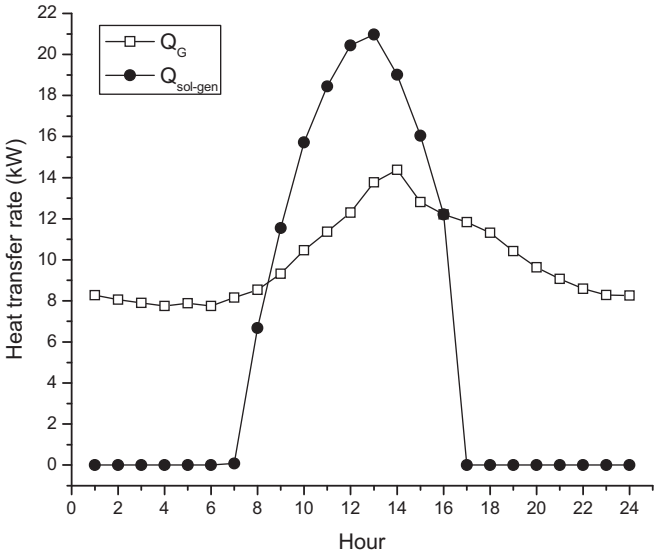

Fig. 16. Comparison of the required heat transfer in the generator (Q_G) and heat production from solar collector ($Q_{sol\text{-}gen}$) during the day for $Q_E = 3.5$ kW.

Fig. 16, the solar heat energy demand in the generator (Q_G) can easily be met by the produced heat energy in the collector ($Q_{sol\text{-}gen}$) from 09:00 to 16:00. According to the obtained results for the cooling capacity value of 3.5 kW, the solar heat energy need in the generator is found to be 9.32 kW while the produced heat energy in the collector is 11.54 kW at 9:00. In addition, both of them are equal to each other with the amount of 12.21 kW at 16:00.

4. Conclusions

This study investigates performance prediction of the usage possibility of the absorption cooling system in the southern region of Turkey for Adana province. It is seen that cooling need and solar radiation variations, which is the greatest advantage of solar-powered cooling system, are overlapping, i.e. the greater the sunshine and thus the cooling load, the larger the cooling effect achieved by the solar refrigerating system. The following discussion and recommendations can be drawn from this investigation:

- One of the most important affecting parameter for the $COP_{cooling}$ of the absorption refrigeration system is the atmospheric air temperature. The $COP_{cooling}$ is inversely proportional to the atmospheric air temperature.
- The COPs fairly change during the day. The $COP_{cooling}$ is in the range of 0.243–0.454 while the $COP_{heating}$ varies from 1.243 to 1.454. The maximum COP occurs during morning hours whereas the minimum COP happens during noon.
- All of the COP values are decreasing with decreasing generator temperature. Specially, the COP becomes considerably low as the generator temperature value is lower than 110 °C. The most suitable performance of the absorption cooling system is calculated for the generator temperature values equal to or higher than 110 °C.
- The maximum solar collector efficiency is calculated as 0.784 at 13:00 for the solar irradiation intensity of 0.719 kW/m^2.
- The condenser capacity is directly proportional to the generator temperature.
- The heat transfer rate in the generator is proportionally increasing with increasing atmospheric air temperature and it takes its maximum value at 14:00 .
- The required collector areas for the evaporator capacities of 2.5, 3.0, 3.5 and 4.0 kW at 16:00 are, in sequence, calculated as 25.68, 30.82, 35.95 and 41.09 m^2. The obtained results show that the solar-powered absorption cooling system requires high performance collectors for the effective operation of the solar-powered absorption cooling and lower collector areas.
- The SAR system is considerably suitable for home/office-cooling purposes between the hours 09:00 and 16:00 in the southern region of Turkey as found for Adana city as well as similar places in the world.

Acknowledgements

The author, Muammer Ozgoren, would like to thank the Coordinatorship of Selcuk University's Scientific Research Office (BAP), Contract No: 09201128.

References

[1] J. Guo, H.G. Shen, Modeling solar-driven ejector refrigeration system offering air conditioning for office buildings, Energy Buildings 41 (2009) 175–181.
[2] H. Esen, M. Inalli, A. Sengur, M. Esen, Artificial neural networks and adaptive neuro-fuzzy assessments for ground-coupled heat pump system, Energy Build. 40 (2008) 1074–1083.
[3] H. Esen, M. Inalli, A. Sengur, M. Esen, Performance prediction of a ground-coupled heat pump system using artificial neural networks, Expert Syst. Appl. 35 (2008) 1940–1948.
[4] H. Esen, M. Inalli, A. Sengur, M. Esen, Forecasting of a ground-coupled heat pump performance using neural networks with statistical data weighting pre-processing, Int. J. Therm. Sci. 47 (2008) 431–441.
[5] C. Koroneos, E. Nanaki, G. Xydis, Solar air conditioning systems and their applicability – an exergy approach, Resour. Conserv. Recycl. 55 (2010) 74–82.
[6] C. Zhang, M. Yang, M. Lu, Y. Shan, J. Zhu, Experimental research on LiBr refrigeration – heat pump system applied in CCHP system, Appl. Therm. Eng. (2011). doi:10.1016/j.applthermaleng.2011.02.004.
[7] A. Sözen, M. Özalp, E. Arcaklioglu, Prospects for utilization of solar driven ejector-absorption cooling system in Turkey, Appl. Therm. Eng. 24 (2004) 1019–1035.
[8] O. Marc, J.P. Praene, A. Bastide, F. Lucas, Modeling and experimental validation of the solar loop for absorption solar cooling system using double-glazed collectors, Appl. Therm. Eng. 31 (2011) 268–277.
[9] S.A. Kalogirou, Solar Energy Engineering: Process and Systems, first ed. Elsevier Ltd. Inc, New York, USA, 2009.
[10] X.Q. Zhai, R.Z. Wang, Experimental investigation and theoretical analysis of the solar adsorption cooling system in a green building, Appl. Therm. Eng. 29 (2009) 17–27.
[11] D.S. Kim, C.A. Infante-Ferreira, Solar refrigeration options – a state-of-the-art-review, Int. J. Refrig. 31 (2008) 3–15.
[12] K. Bakirci, B. Yuksel, Experimental thermal performance of a solar source heat-pump system for residential heating in cold climate region, Appl. Therm. Eng. 31 (2011) 1508–1518.
[13] V.G. Gude, N. Nirmalakhandan, Sustainable desalination using solar energy, Energy Convers. Manage. 51 (2010) 2245–2251.
[14] R. Mastrullo, C. Renno, A thermoeconomic model of a photovoltaic heat pump, Appl. Therm. Eng. 30 (2010) 1959–1966.
[15] F. Assilzadeh, S.A. Kalogirou, Y. Ali, K. Sopian, Simulation and optimization of a LiBr solar absorption cooling system with evacuated tube collectors, Renew. Energy 30 (2005) 1143–1159.
[16] J. Sun, L. Fu, S. Zhang, W. Hou, A mathematical model with experiments of single effect absorption heat pump using LiBr–H_2O, Appl. Therm. Eng. 30 (2010) 2753–2762.
[17] J. Sun, L. Fu, S. Zhang, Performance calculation of single effect absorption heat pump using LiBr + $LiNO_3$ + H_2O as working fluid, Appl. Therm. Eng. 30 (2010) 2680–2684.
[18] J.R. García Cascales, F. Vera García, J.M. Cano Izquierdo, J.P. Delgado Marín, R. Martínez Sánchez, Modelling an absorption system assisted by solar energy, Appl. Therm. Eng. 31 (2011) 112–118.
[19] B.H. Gebreslassie, G. Guillén-Gosálbez, L. Jiménez, D. Boer, Economic performance optimization of an absorption cooling system under uncertainty, Appl. Therm. Eng. 29 (2009) 3491–3500.
[20] D. Hong, L. Tang, Y. He, G. Chen, A novel absorption refrigeration cycle, Appl. Therm. Eng. 30 (2010) 2045–2050.
[21] C. Monné, S. Alonso, F. Palacín, L. Serra, Monitoring and simulation of an existing solar powered absorption cooling system in Zaragoza (Spain), Appl. Therm. Eng. 31 (2011) 28–35.
[22] A.A. Manzela, S.M. Hanriot, L. Cabezas-Gómez, J.R. Sodré, Using engine exhaust gas as energy source for an absorption refrigeration system, Appl. Energy 87 (2010) 1141–1148.

[23] D.S. Kim, Solar Absorption Cooling, Master of Mechanical Engineering, Korea University, 2007.
[24] L. Garousi Farshi, S.M. Seyed Mahmoudi, M.A. Rosen, Analysis of crystallization risk in double effect absorption refrigeration systems, Appl. Therm. Eng. 31 (2011) 1712–1717.
[25] S.A. Kalogirou, Solar thermal collectors and applications, Prog. Energy Combust. Sci. 30 (2004) 231–295.
[26] R. Yamankaradeniz, I. Horuz, O. Kaynakli, S. Coskun, N. Yamankaradeniz, Refrigeration Techniques and Heat Pump Applications, second ed. Dora Publication Company, Bursa, Turkey, 2009, (in Turkish).
[27] S. Kalogirou, Recent patents in solar energy collectors and applications, Recent Patents Eng. 1 (2007) 23–33.
[28] C. Beggs, Energy: Management, Supply and Conservation, second ed. Elsevier Ltd. Inc, Burlington, USA, 2009.
[29] Thermo Dynamics Ltd, www.thermo-dynamics.com/pdfiles/technical/ETC_v_LFP.pdf, (accessed 01.05.11), pp. 1–4.
[30] H. Esen, F. Ozgen, M. Esen, A. Sengur, Artificial neural network and wavelet neural network approaches for modelling of a solar air heater, Expert Syst. Appl. 36 (2009) 11240–11248.
[31] H. Esen, F. Ozgen, M. Esen, A. Sengur, Modelling of a new solar air heater through least-squares support vector machines, Expert Syst. Appl. 36 (2009) 10673–10682.
[32] M. Esen, Thermal performance of a solar cooker integrated vacuum-tube collector with heat pipes containing different refrigerants, Solar Energy 76 (2004) 751–757.
[33] M. Esen, H. Esen, Experimental investigation of a two-phase closed thermosyphon solar water heater, Solar Energy 79 (2005) 459–468.
[34] I. Pilatowsky, W. Rivera, J.R. Romero, Performance evaluation of a monomethylamine-water solar absorption refrigeration system for milk cooling purposes, Appl. Therm. Eng. 24 (2004) 1103–1115.
[35] M. Mazloumi, M. Naghashzadegan, K. Javaherdeh, Simulation of solar lithium–water absorption cooling system with parabolic trough collector, Energy Convers. Manage. 49 (2008) 2820–2832.
[36] R.J. Romero, W. Rivera, I. Pilatowsky, R. Best, Comparison of the modeling of a solar absorption system for simultaneous cooling and heating operating with an aqueous ternary hydroxide and with water/lithium bromide, Solar Energy Mater. Solar Cell 70 (2001) 301–308.
[37] H. Vidal, S. Colle, G. dos Santos Pereira, Modelling and hourly simulation of a solar ejector cooling system, Appl. Therm. Eng. 26 (2006) 663–672.
[38] Y.A. Cengel, M.A. Boles, Thermodynamics: An Engineering Approach, fifth ed. McGrawHill, New York, USA, 2008.
[39] H.K. Ersoy, S. Yalcin, R. Yapici, M. Ozgoren, Performance of a solar ejector cooling-system in the southern region of Turkey, Appl. Energy 84 (2007) 971–983.
[40] J.A. Duffie, W.A. Beckman, Solar Engineering of Thermal Processes, John Wiley & Sons Inc, New York, USA, 1980.
[41] M. Ozgoren, O. Solmaz, A. Kahraman, Determination of cooling load of a midibus via meteorological data: Case Study For Edirne. International Scientific Conference, UNITECH09, 20–21 November 2009, Gabrovo, Bulgaria, 544–551.
[42] C.P. Jacovides, F.S. Tymvios, V.D. Assimakopoulos, N.A. Kaltsounides, Comparative study of various correlations in estimating hourly diffuse fraction of global solar radiation, Renew. Energy 31 (2006) 2492–2504.
[43] G. Notton, P. Poggi, C. Cristofari, Predicting hourly solar irradiations on inclined surfaces based on the horizontal measurements: performances of the association of well-known mathematical models, Energy Convers. Manage. 47 (2006) 1816–1829.